

Solar-Biomass Driven Ejector Refrigeration System

Mark Anthony B. Redo, Menandro S. Berana

Abstract— Ejector cooling systems basically utilize low-grade thermal energy from waste heat or renewable energy sources. In this study, solar thermal coupled to biomass energy as two abundant Philippine resources were employed in the system. Heating capacity of the combined sources provided the varying generating temperature of the working fluid from 60 °C to 100 °C. At this varying condition, condensing temperature is projected at a constant evaporating temperature. The system performance is observed along the varying generating and evaporating temperatures. Two natural working fluids, which are ammonia and R134a, were used in the calculation.

The mathematical modelling was established with focus on the ejector. The fluid and flow properties were numerically solved by applying the conservation equations with an account of the frictional losses. Moreover, superheated and two-phase flow simulations were included. After numerical analyses, entrainment ratio was fixed at 0.30, and the coefficient of performance, an important non-dimensional parameter, was at the range of 0.24 to 0.30. The nozzle and ejector efficiencies were very high at a range from 93% to 99%. The ejector profiles were projected and the area ratio that relates the nozzle and the mixing geometry were from 3.98 to 9.23. Between the fluids, ammonia gave the higher coefficient of performance (COP) with higher refrigerating capacity at a lower heat input and better efficiency than R134a. It also produced smaller optimized ejector dimensions.

Keywords—ejector, cooling system, solar, biomass

I. Introduction

A big percentage of the annual global primary energy consumption comes from oil, coal and natural gas [1]. They are fossil fuels formed by natural processes; and this means that they are subject to depletion [2]. Numerous researchers are forecasting its near-term peak and eventual depletion [3, 4].

In the Philippines, the 2010 fossil fuel consumption for power generation was 74%. The largest consumers are residential, industrial and commercial sectors where a huge percentage of their electricity usage goes to air conditioning and refrigerating needs [5]. On one hand, the country depends on vapor compression refrigeration systems where high power is required. On the other hand, high volume of low-grade heat from renewable energies and waste heat are available. One of which is the solar energy. The country receives an average solar radiation of 161.7 watts per sq. m. since its location is just above the equator and longer summer period is experienced [5].

Mark Anthony B. Redo, Menandro S. Berana
Department of Mechanical Engineering, University of the Philippines-Diliman
Philippines

A potential solar generation of 4.5 to 5.5 kW-h per sq. m. per day presented in Fig. 1 was recorded by the Philippine Department of Energy (DOE) together with the US National Renewable Energy Laboratory (NREL) applying the Climatological Solar radiation (CSR) model [6]. Additionally, the Philippines as an agricultural country produces an abundant amount of biological wastes mainly from by-products and residues of growing crops. Huge quantities of these are abandoned and untapped as reported by Baconguis [7] and specified in Table 1. With the abundance of solar and biomass resources, heat-driven cooling systems are a good solution in reducing primary energy consumptions.

One of the economically feasible refrigeration systems that harness low-grade thermal energy is the ejector refrigeration system (ERS). It offers some advantages over absorption and adsorption refrigeration systems. To mention, ERS has lower initial cost, robust, long lifespan, with simplistic structure and is satisfactorily working at lower heat source temperatures [8]. When compared to the conventional vapor refrigeration system, ERS helps in alleviating environmental problems because equivalent CO₂ emission from power generation can be reduced as the compressor is eliminated. Additionally, natural refrigerants that have very low or zero ozone depleting potential (ODP) and global warming potential (GWP) can be utilized to have benign impact to the environment.

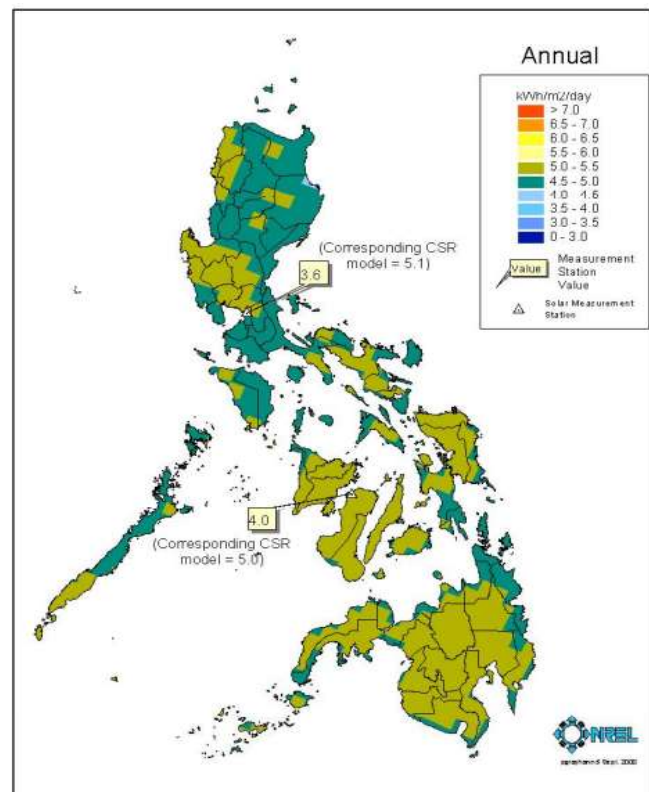


Figure 1. Philippine average solar resource. (source: NREL [6])

TABLE I. PHILIPPINE ABANDONED BIOMASS
(SOURCE: BACONGUIS [7])

Product	Total (x1000 metric tons)
Rice Hull	2357.325
Bagasse	5985839.549
Coco-Shell	1948.867
Coconut Husk	4330.814
Coco-Coir	3031.57
Jatropha	300

II. Numerical Scheme

A. Cycle Modelling

The basic components of an ERS, as illustrated through the schematic diagram in Fig. 2 and the temperature-entropy ($T-s$) in Fig. 3, are (1) ejector, (2) vapor generator, (3) condenser, (4) evaporator, (5) pump and (6) expansion device. The heat input Q_g enters the vapor generator so that the liquid refrigerant is vaporized. This high pressure, high temperature primary fluid \dot{m}_p enters the ejector, which causes entrainment for the secondary fluid \dot{m}_s . The two high speed flows mix together and the pressure energy is regained after passing through the diffuser part of the ejector. The total flow \dot{m}_m condenses as it rejects heat Q_c to the environment. At saturated liquid state, the primary flow is pumped back to the vapor generator, while the secondary flow is expanded and produces refrigerating effect Q_e at the evaporator.

The energy balance was simply applied on the heat exchangers to measure the corresponding heat absorbed or rejected by the refrigerant.

$$Q_g = \dot{m}_p (h_2 - h_1) \quad (1)$$

$$Q_c = \dot{m}_m (h_4 - h_5) \quad (2)$$

$$Q_e = \dot{m}_s (h_3 - h_6) \quad (3)$$

The equation for the pump work is as follows:

$$W_p = \dot{m}_p (h_1 - h_5) \quad (4)$$

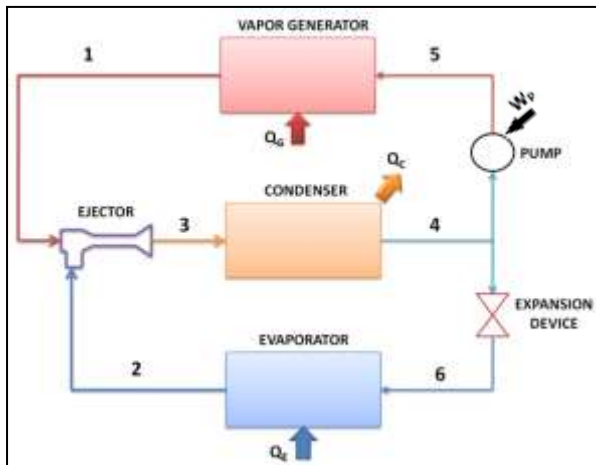


Figure 2. ERS schematic diagram.

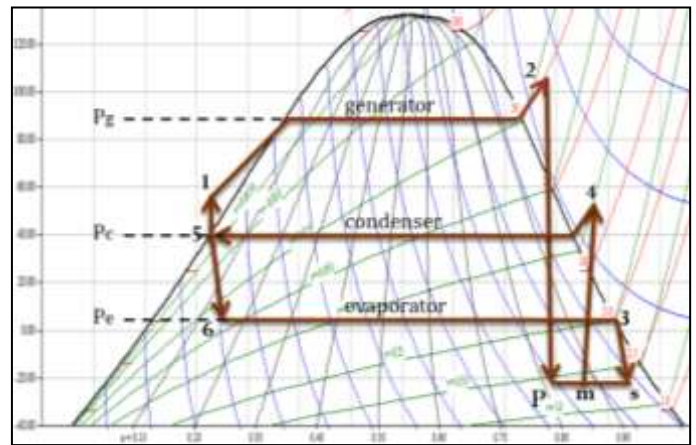


Figure 3. $T-s$ diagram of the ERS

One of the important performance parameters of the ERS is the entrainment ratio [9]. This is the ratio of the secondary mass flow rate over the primary flow rate. This is also related to the system performance.

$$\omega = \frac{\dot{m}_s}{\dot{m}_p} \quad (5)$$

In addition, the efficiency of the system is monitored from the coefficient of performance (COP). For a heat-driven refrigeration system, this is expressed by the ratio of the refrigerating capacity over the heat input at the vapor generator

$$COP = \frac{Q_e}{Q_g} \quad (6)$$

It is also a function of the entrainment ratio and the change of enthalpies through the evaporator and the generator.

$$COP = \frac{\dot{m}_s \Delta h_e}{\dot{m}_p \Delta h_g} = \omega \left(\frac{\Delta h_e}{\Delta h_g} \right) \quad (7)$$

B. Ejector Modelling

The heart of the ERS is the ejector; thus, it requires careful modelling and analysis to come up on the desired cooling [10]. These assumptions were brought out in the establishment of the mathematical model of the ejector [11–16]: (1) homogenous fluid flow; (2) steady-state and one-dimensional flow; (3) irreversible flow processes are considered where entropy generation is due to frictional losses; (4) adiabatic process is also considered; and (5) phase change is accounted, and equilibrium is assumed for the liquid and vapor phases.

Fundamental concepts of thermodynamics and conservation equations are employed on the modelling of every ejector section shown in Fig. 4 together with the resulting pressure and velocity profiles of the fluid flow. Suggestions of ASHRAE [17] and ESDU [18] on geometry of ejector components are used. The properties of the working fluid are determined through REFPROP 8.0 [19] which uses

the data determined by the National Institute of Standards and Technology (NIST).

III. Results and Discussions

The vapor generator used is a counter flow plate heat exchanger (PHE) which fits the application and demonstrates significant advantages [20]. The solar-thermal coupled to biomass heat input is varied for the generating temperature of the refrigerant from 60°C to 100°C. The performance of the system is evaluated and compared using two commonly employed fluids, R134a and ammonia [21]. Moreover, a 3-degree C superheat is added to the generating condition before the inlet of the nozzle.

The relationship of the generating temperature with the condensing temperature and heat input is presented in Fig. 5. It can be seen that as the generating temperature increases at a fixed mass flow rates or entrainment ratio of 0.30 and evaporating temperature, the condensing temperature also increases. This is because a higher generating temperature means longer fluid expansion at the primary nozzle, which results to a higher recompression that affects the condensation. However, lowering the evaporating temperature causes a decrease in the condensing temperature with the same increasing trend for generating temperature. Thus, condition is achieved at low evaporating temperature.

The required heat input from solar-biomass heat sources decreases at an increasing generating temperature. This is because the temperature difference for the heat requirement Q_g drops due to higher condensing temperature. Yet, for a lower evaporating temperature or larger cooling needs, greater heat input is required as shown in Fig. 5. R134a fluid necessitates high heat input than ammonia for the same working temperatures.

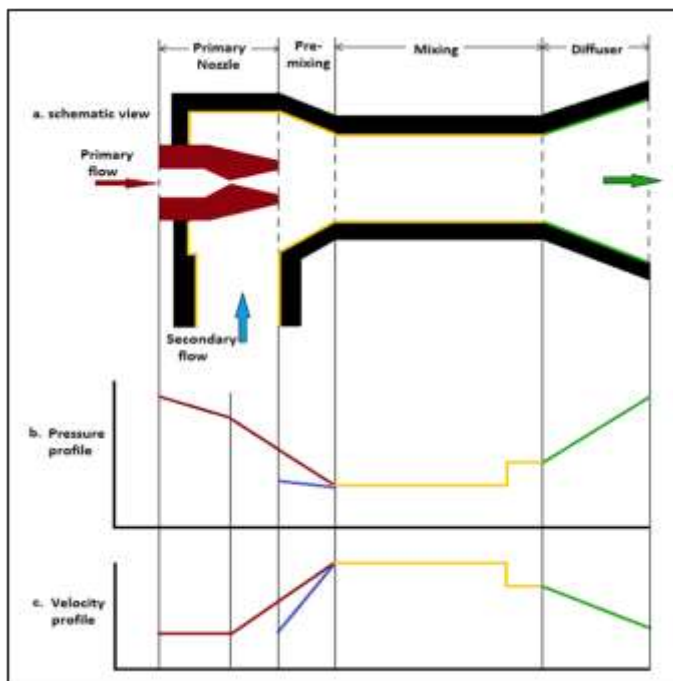


Figure 4. Ejector sections and profile.

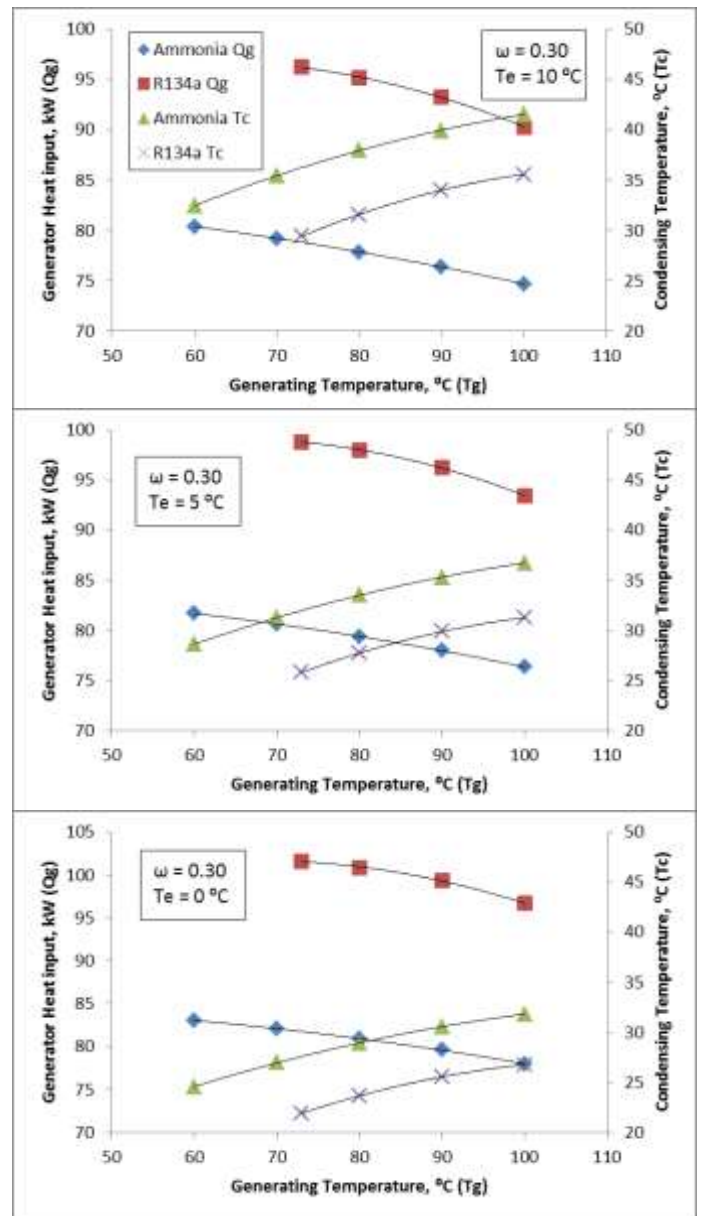


Figure 5. Effect of generating temperature to heat input and condensing temperature.

Fig. 6 illustrates the effect of varying the generating temperature for each set of fixed evaporating temperature at 10°C, 5°C and 0°C. Refrigerating effect observably decreases with the increase in generating temperature, though the trend basically increases with a decrease in evaporating temperature from 22 kW to 25 kW. For ammonia, the COP slowly increases with increasing generating temperature while R134a exhibits gradual decrease down to 85 °C and then rises again to 100 °C. The slow change is caused by the gradual variation of heat input and refrigerating capacity. It is also worth noting that the ERS has low COP since it is a heat-driven system and such heat is low-grade, abundantly available and free.

The efficiencies of the nozzle and the ejector are presented in Fig. 7 along with the generating temperature. A decrease in the nozzle efficiency occurs as the generating temperature

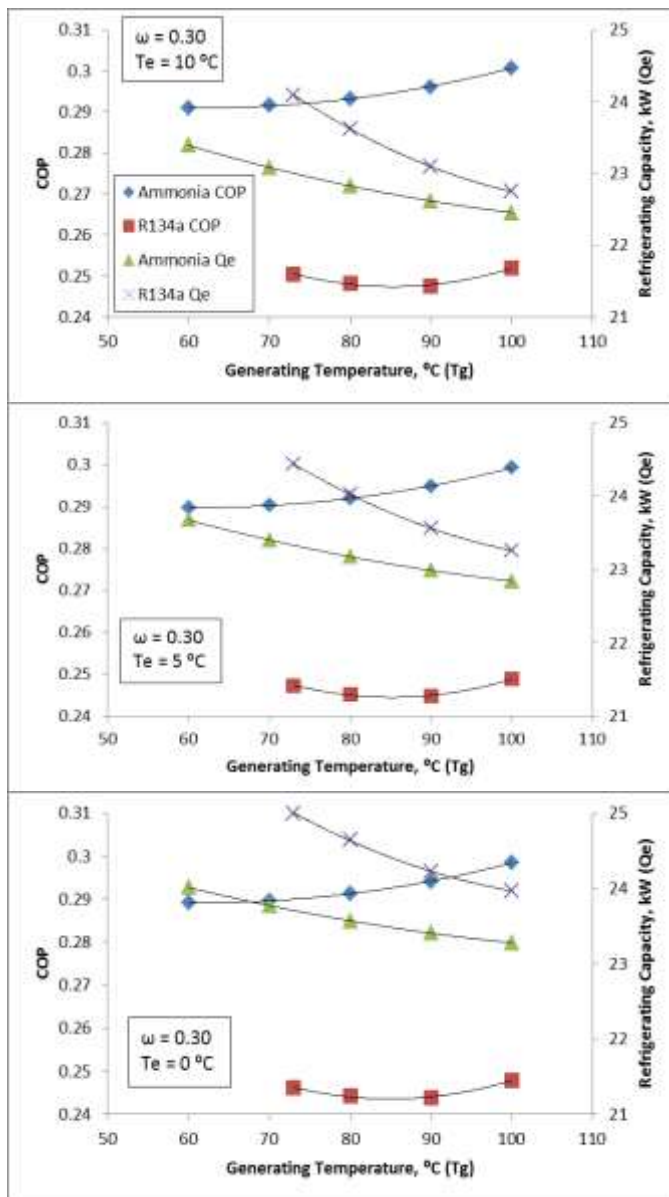


Figure 6. Effect of generating temperature to COP and refrigerating capacity.

increases. Primarily, this happens because of the nozzle expansion. As the generating temperature goes higher at a constant evaporating temperature, nozzle length becomes longer. This also means that additional frictional losses accounted to the efficiency. Meanwhile, ammonia demonstrates better ejector efficiency than R134a which might be because the former has better transport properties. However, the efficiencies are still higher from 90 to 99% for both the nozzle and the ejector for the two fluids. This is mainly due to the fact that entire ejector has no moving parts. Hence, high efficiency and effectiveness are achieved.

Based on the evaporating temperature fixed at 5°C , entrainment ratio at 0.30 and degree of superheat at 3°C , the optimized ejector geometry is determined as shown in Table 2 for different generating temperatures. For ammonia, it is from

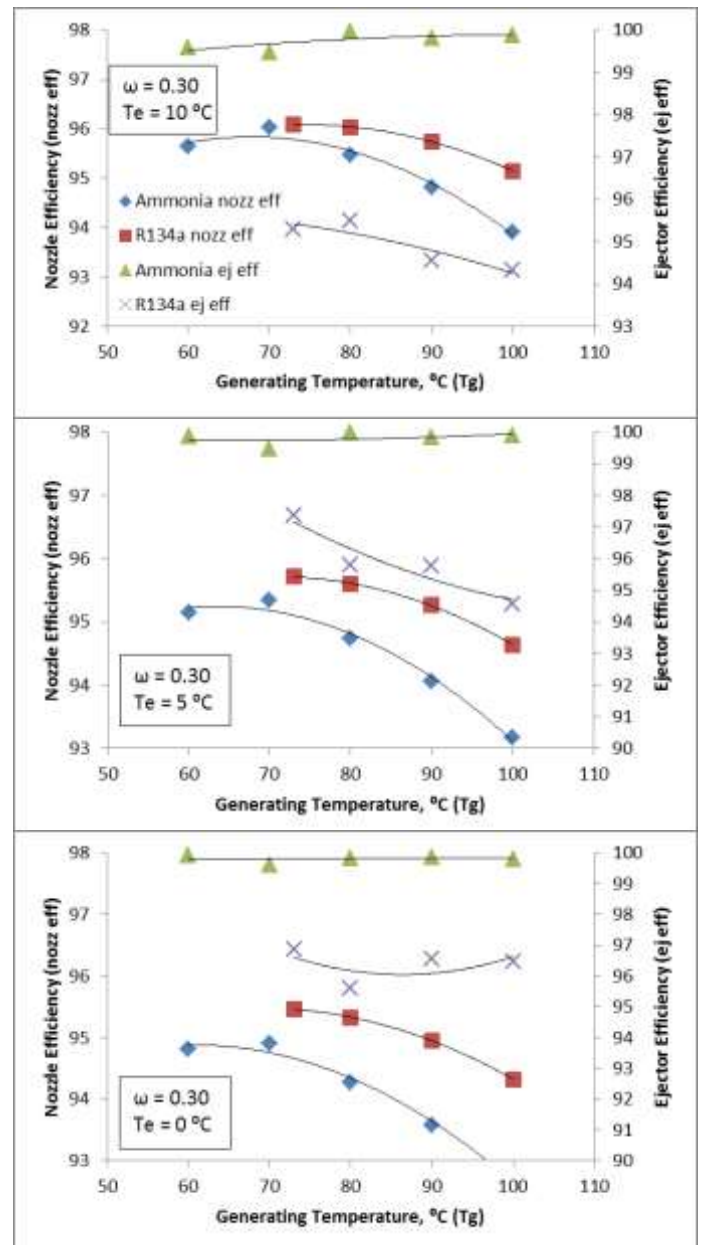


Figure 7. Effect of generating temperature to nozzle and ejector Efficiency.

60°C to 100°C , while for R134a, the lowest generating temperature that works at the operating conditions is at 73°C . The maximum temperature is at 100°C , just below the critical temperature of R134a. The geometrical measures correspond to the profile in Fig. 8.

The area ratio (AR) which is defined as the ratio of the cross-sectional area of the mixing chamber and the cross-sectional area of the throat of the primary nozzle is a significant parameter. This non-dimensional measure relates the primary nozzle, the entrainment of the secondary flow, as well as the mixing of two flows with the geometrical area. As shown in Table 2, this yields higher value as the generating temperature goes higher as well.

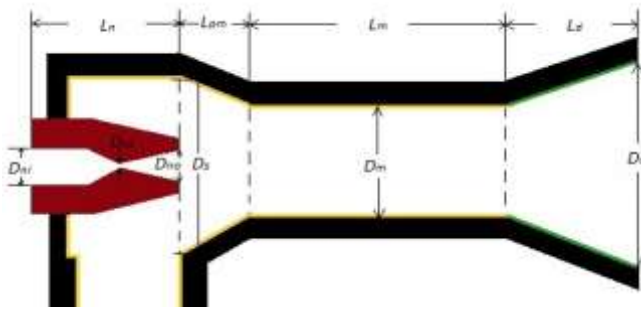


Figure 8. Ejector profile.

References

- [1] U.S. Energy Information Administration, <http://www.eia.gov/> (October 2008).
- [2] C. J. Campbell, “Recognising the second half of the oil age,” *Environmental Innovation and Societal Transitions*, vol. 9, pp. 13–17, 2013.
- [3] M. Hook, “Depletion rate analysis of fields and regions: A methodological foundation,” *Fuel*, vol. 121, pp. 95-108, 2014.
- [4] S. Sorrell, J. Speirs, R. Bentley, A. Brandt, R. Miller, “Global oil depletion: A review of evidence,” *Energy Policy*, vol. 38, pp. 5290–95, 2010.
- [5] Department of Energy (DOE) Philippines, Energy Center, Rizal Drive, Bonifacio Global City, Taguig City, Philippines 1632, <http://www.doe.gov.ph/>, 2010-2013.
- [6] D. Renne, P. Gray-Hann, R. George, L. Brady, Assessment of solar resources in the Philippines, NREL under US Agency for International Development, 2000.
- [7] R. Bacongus, Abandoned biomass resource statistics in the Philippines, 10th National Convention on Statistics (NCS), EDSA Shangri-La Hotel, October 1–2, 2007.
- [8] T. Sankaral, A. Mani, “Experimental studies on an ammonia ejector refrigeration system,” *International Communications in Heat and Mass Transfer*, vol. 33, pp. 224–230, 2006.
- [9] K. Pianthong, W. Seehanam, M. Behnia, T. Sriveerakul, S. Aphornratana, “Investigation and improvement of ejector refrigeration system using computational fluid dynamics technique,” *Energy Conversion and Management*, vol. 48, pp. 2556–64, 2007.
- [10] J. M. Abdulateef, K. Sopian, M. A. Alghoul, M. Y. Sulaiman, “Review on solar-driven refrigeration technologies,” *Renewable and Sustainable Energy Reviews*, vol. 13, pp. 1338–49, 2009.
- [11] M. A. B. Redo, Design and experimental analysis of heat-driven ejector refrigeration system, Master’s Thesis, University of the Philippines Diliman, 2014.
- [12] G. D. Espeña, Heat-driven ejector refrigeration system for hot-spring resorts application, Master’s Thesis, University of the Philippines Diliman, 2014.
- [13] M. A. B. Redo, M. S. Berana, G. D. Espeña, Mathematical model of irreversible nozzle condition for heat-driven ejector refrigeration system, Proceedings of the 8th International Conference on Multiphase Flow (ICMF 2013), Jeju, Korea, May 26 – 31, 2013.
- [14] M. S. Berana, Characteristics and shock waves of supersonic two-phase flow of CO₂ through converging-diverging nozzles, Doctoral Dissertation, Toyohashi University of Technology, Toyohashi, Aichi, Japan, 2009.
- [15] M. S. Berana, E. T. Bermido, Design and analysis of ejector powerplant system, Proceedings of the ASME 2013 International Mechanical Engineering Congress and Exposition (IMECE2013), San Diego, California, USA, November 15–21, 2013.
- [16] M. S. Berana, E. T. Bermido, Ejector modelling for powerplant application, Proceedings of the 8th International Conference on Multiphase Flow (ICMF 2013), Jeju, Korea, May 26–31, 2013.
- [17] ASHRAE, Steam-jet refrigeration equipment, *Equipment Handbook*, vol.13, pp. 13.1–13.6, 1979.
- [18] ESDU, Ejectors and jet pumps, design for steam driven flow, Engineering Science Data item 86030, Engineering Science Data Unit, London, 1986.
- [19] E. W. Lemmon, M. L. Huber, M. O. McLinden, NIST Standard Reference Database 23: Reference Fluid Thermodynamic and Transport Properties - REFPROP, Version 8.0, National Institute of Standards and Technology, 2007.
- [20] J. Gut, J. Pinto, “Optimal configuration design for plate heat exchangers,” *International Journal of Heat and Mass Transfer*, vol. 47, pp. 4833–4848, 2004.
- [21] X. Chen, S. Omer, M. Worall, S. Riffat, “Recent developments in ejector refrigeration technologies,” *Renewable and Sustainable Energy Reviews*, vol. 19, pp. 629–651, 2013.

TABLE II. OPTIMIZED EJECTOR DIMENSIONS (in mm) AT $T_e=5^\circ\text{C}$, $\omega=0.3$, DEG. SUP.= 3°C

Ammonia													
Tg (°C)	Qe (kW)	Dni	Dt	Dno	Ds	Dm	Dd	Ln	Lpm	Lm	Ld	Ltot	AR
60	23.67	39.99	4.61	5.99	31.22	9.29	41.36	14.94	2.83	92.91	90.94	201.6	3.98
70	23.40	35.24	4.09	5.74	31.17	9.11	30.65	14.90	2.87	91.11	61.08	169.9	4.98
80	23.17	31.15	3.64	5.55	31.13	8.97	53.54	14.83	2.91	89.73	126.4	233.8	6.15
90	22.99	27.58	3.26	5.41	31.10	8.86	38.28	14.74	2.92	88.60	83.44	189.6	7.49
100	22.84	24.40	2.92	5.28	31.07	8.75	42.42	14.63	2.91	87.54	95.48	200.5	9.06
R134a													
Tg (°C)	Qe (kW)	Dni	Dt	Dno	Ds	Dm	Dd	Ln	Lpm	Lm	Ld	Ltot	AR
73	24.44	43.66	8.44	11.90	42.13	18.82	42.16	22.47	5.71	188.2	66.16	282.5	4.97
80	24.03	39.63	8.11	11.81	42.12	18.81	37.93	23.53	5.84	188.1	54.22	271.6	5.84
90	23.56	34.25	7.13	11.73	42.10	18.82	37.99	24.95	6.01	188.1	54.36	273.5	7.37
100	23.26	29.07	6.29	11.60	42.07	18.75	35.79	25.91	6.10	187.5	48.31	267.8	9.23

iv. Conclusion

With the abundance of solar radiation received by the Philippines and with the large quantity of abandoned biomass, heat-driven ERS offers utilization possibility for different cooling needs. For instance, agricultural products and post harvests can be supported by this refrigeration system. Moreover, comfort cooling of buildings and establishments can adopt and benefit from this. ERS is also economically competitive since its operation cost will be very low. There is no compressor, and pump requires less amount of electricity.

After investigating the performance of the two fluids, ammonia demonstrates higher COP, lower heat input to produce higher refrigerating capacity and better nozzle and ejector efficiencies. It also yields a smaller set of optimized ejector geometry compared with that of R134a.

Acknowledgment

This study had been completed and is disseminated through the support of Engineering Research and Development for Technology program of the Department of Science and Technology of the Republic of the Philippines.